Insect Molecular Biology

Insect Molecular Biology (2011) **20**(5), 675–685 doi: 10.1111/j.1365-2583.2011.01100.x

Development of a novel set of Gateway-compatible vectors for live imaging in insect cells

G. A. Maroniche, V. C. Mongelli, V. Alfonso, G. Llauger, O. Taboga and M. del Vas

Instituto de Biotecnología, CICVyA, Instituto Nacional de Tecnología Agropecuaria (IB-INTA), Las Cabañas y Los Reseros, Hurlingham, Buenos Aires, Argentina

Abstract

Insect genomics is a growing area of research. To exploit fully the genomic data that are being generated, high-throughput systems for the functional characterization of insect proteins and their interactomes are required. In this work, a Gateway-compatible vector set for expression of fluorescent fusion proteins in insect cells was developed. The vector set was designed to express a protein of interest fused to any of four different fluorescent proteins [green fluorescent protein (GFP), cyan fluorescent protein (CFP), yellow fluorescent protein (YFP) and mCherry] by either the C-terminal or the N-terminal ends. Additionally, a collection of organelle-specific fluorescent markers was assembled for colocalization with fluorescent recombinant proteins of interest. Moreover, the vector set was proven to be suitable for simultaneously detecting up to three proteins by multiple labelling. The use of the vector set was exemplified by defining the subcellular distribution of *Mal de Río Cuarto virus* (MRCV) outer coat protein P10 and by analysing the *in vivo* self-interaction of the MRCV viroplasm matrix protein P9-1 in Förster resonance energy transfer (FRET) experiments. In conclusion, we have developed a valuable tool for high-throughput studies of protein subcellular localization that will aid in the elucidation of the function of newly described insect and virus proteins.

Correspondence: Mariana del Vas, PhD, Instituto de Biotecnología, CICVyA, Instituto Nacional de Tecnología Agropecuaria (IB-INTA), Las Cabañas y Los Reseros s/n. Hurlingham CP 1686, Buenos Aires, Argentina. Tel.: + 005411 4621 1676; fax: + 005411 4621 0199; e-mail: mdelvas@cnia.inta.gov.ar

Keywords: live imaging, insect, gateway, GFP, *Mal de Río Cuarto virus*.

Introduction

In order to provide a comprehensive view of the functional structure of living organisms, it is important to integrate the overwhelming amount of data that is being produced as a result of transcriptomic, proteomic and metabolomic large-scale studies. To accomplish this, it is essential to identify and understand protein function and to decipher interaction networks, most of which in the first instance rely on subcellular protein distribution. Although it is possible to predict the subcellular localization of a newly identified protein *in silico* (Eisenhaber & Bork, 1998), an experimental confirmation is required. When working at high throughput, the expression of tagged proteins in cells is a fast and efficient approach that also preserves physiological conditions. The introduction of fluorescent proteins (FPs) into the research field was a major breakthrough in biology that opened the possibility for complex studies in living cells. After the isolation of the jellyfish *Aequorea victoria* green fluorescent protein (GFP) (Prasher *et al*., 1992), and the anemone *Discosoma striata* red fluorescent protein (DsRed) (Matz *et al*., 1999), a wide variety of FPs derivates, covering most of the visible spectrum was engineered for improved brightness, photostability and quantum yield (reviewed by Shaner *et al*., 2007). Even though the most extensively used are the enhanced version of GFP (EGFP) (Heim *et al*., 1995), ECFP, EYFP (Heim *et al*., 1994) and the red mCherry protein (Shaner *et al*., 2004), the variety of FPs is astonishing and growing every day together with the diversity of their possible uses in research (Cole *et al*., 1996; Miyawaki *et al*., 1999; Wouters & Bastiaens, 1999; Hu *et al*., 2002; Hanson *et al*., 2004; Shcherbo *et al*., 2007; Wong *et al*., 2007). Particularly, the use of FPs as fusion partners for protein subcellular localization in living cells is one of the most powerful and suitable approaches for rapid exploration of protein function (Day & Schaufele, 2005; Pepperkok & Ellenberg, 2006).

As a result of insects' fundamental roles in ecology and agriculture, insect molecular and cellular biology is a growing field of research that is rapidly advancing with the genome sequencing of several important insects (Adams *et al*., 2000; Holt *et al*., 2002; Mita *et al*., 2004; Xia *et al*., 2004; Consortium, 2006, 2010; Nene *et al*., 2007; Richards *et al*., 2008; Kirkness *et al*., 2010; Werren *et al*., 2010). The thorough exploitation of this growing genomic information will require the development of new high-throughput systems specially designed for insects. In fact, a two hybrid system in insect cells (Mon *et al*., 2009) and a series of vectors for high-level protein expression in lepidopteran cells (Lee *et al*., 2008) have been already reported.

In this work we developed a novel set of vectors for *in vivo* subcellular localization of proteins in insect cell lines, which is compatible with the fast and easy Gateway cloning technology (Invitrogen, Carlsbad, CA, USA). The deployment of such vectors was demonstrated by resolving the subcellular localization of the outer capsid protein P10 of *Mal de Río Cuarto virus* (MRCV) and by establishing the *in vivo* self-interaction of MRCV viroplasm matrix protein P9-1 in Förster resonance energy transfer (FRET) experiments. This new vector set constitutes a valuable research tool for high-throughput protein studies in insect cell cultures.

Results

Construction and assessment of a set of novel Gateway-compatible vectors for live imaging in insect cells

A series of vectors useful to study the subcellular localization of proteins in insect cells was constructed. The pIB-V5/His-Destination (DEST) vector (Invitrogen) was modified by inserting GFP, cyan fluorescentprotein (CFP), yellow fluorescent protein (YFP) or mCherry coding sequences at either the 5′ or the 3′ ends of a Gateway cassette in the proper coding frame to achieve their respective N- or C-terminal fusions to proteins of interest by recombinational cloning. The four destination vectors designed for N-terminal fusions were named pIB-GW, pIB-CW, pIB-YW and pIB-RW (Fig. 1), where G, C, Y and R correspond to GFP, CFP, YFP and mCherry, respectively, and W indicates the Gateway cassette in its actual position respective to each FP sequence. Accordingly, the four destination vectors designed for C-terminal fusions were named pIB-WG, pIB-WY, pIB-WC and pIB-WR (Fig. 1). The correct assembly of the sequences in the vectors was verified by sequencing.

Next, the proper functionality of the vectors was tested using the MRCV viroplasm matrix protein P9-1 (Maroniche *et al*., 2010). The eight destination vectors described above were used in recombination reactions to obtain expression vectors coding for the fluorescent fusion proteins GFP:P9-1, CFP:P9-1, YFP:P9-1, mCherry:P9-1, P9-1:GFP, P9-1:CFP, P9-1:YFP and P9-1:mCherry. These fluorescent chimeric proteins were expressed in *Spodoptera frugiperda* Sf9 cells (Sf9) cells and their distribution pattern was studied by fluorescent live imaging. The N-terminal fusions GFP:P9-1, CFP:P9-1 and YFP:P9-1 were able to form inclusion bodies similar to those reported for MRCV P9-1 protein (Maroniche *et al*., 2010), although the mCherry:P9-1 fusion was evenly distributed in the cytoplasm showing some diffuse accumulations (Fig. 2A). Similarly, the C-terminal fusions P9-1:GFP, P9-1:CFP and P9-1:YFP formed conspicuous and bright cytoplasmic viroplasm-like structures and the P9-1:mCherry tended to be dispersed across the cytoplasm with some subtle accumulations (Fig. 2B). The transfection efficiency of all these vectors was approximately 40% and similar to the efficiency of a construct derived from the same parental vector (Maroniche *et al*., 2010). In sum, all vectors were functional and allowed the expression of fluorescent fusions of a protein of interest in insect cells.

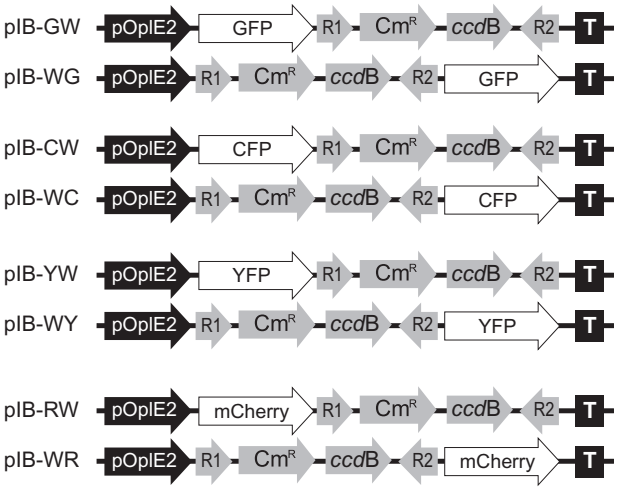

Figure 1. Schematic representation of the Gateway destination vectors constructed in this work. Black features represent the *Orgyia pseudotsugata* nuclear polyhedrosis virus immediate-early 2 gene promoter (pOpIE2) and the transcriptional terminator sequence containing the OpIE2 polyadenylation signal (T). Grey features indicate components of the Gateway recombinational cassette: the attR1 (R1) and attR2 (R2) recombination sites, the chloramphenicol resistance gene (CmR) and the toxic *ccd*B gene. White features correspond to the coding sequences of the different fluorescent proteins. CFP, cyan fluorescent protein; GFP, green fluorescent protein; YFP, yellow fluorescent protein.

Assembly and evaluation of a series of fluorescent organelle markers for colocalization studies

The unambiguous subcellular localization of a given protein by live imaging requires organelle markers for colocalization studies. In order to assemble a collection of

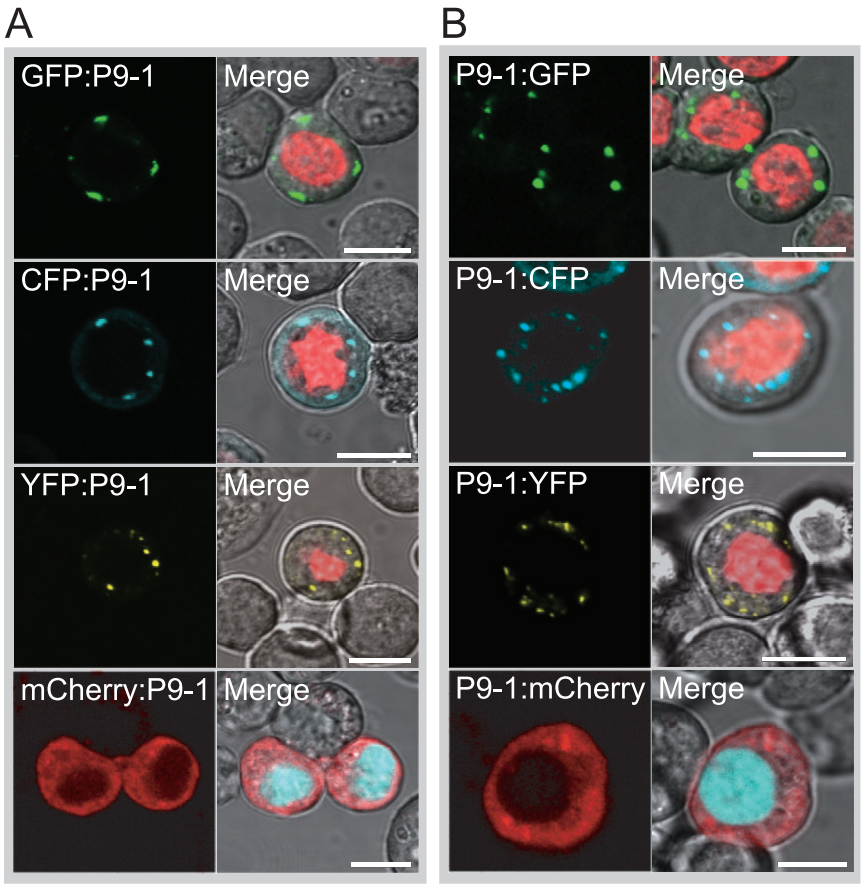

Figure 2. Live imaging of *Spodoptera frugiperda* Sf9 cells (Sf9) expressing different *Mal de Río Cuarto virus* (MRCV) P9-1 fluorescent fusions. (A and B) The vector set constructed in this work was used to obtain P9-1 N-terminal (A) and C-terminal (B) fusions to green fluorescent protein (GFP), cyan fluorescent protein (CFP), yellow fluorescent protein (YFP) and mCherry. All the fluorescent fusions were transiently expressed in Sf9 cells and their subcellular distribution was analysed by confocal microscopy. For each case, the image of the P9-1 fluorescent fusion (left panel) and its merging with images of a nuclear marker [*Homo sapiens* lamin C (LMNA1):mCherry or LMNA1:CFP] and the bright field (right panel) are shown. Scale bars = 10 μm.

reference fluorescent organelle markers appropriate for insect cells, entry vectors containing the coding region of *Homo sapiens* lamin C (LMNA) lacking the first 150 amino acids, *H. sapiens* KDEL endoplasmic reticulum retention receptor 1 (KDELR1), *H. sapiens trans* Golgi network protein 2 (TGOLN2), *H. sapiens* phospholipase A2 (PLA2G15), *Rattus norvegicus* torsin A interacting protein 1 (TOR1AIP1) and *R. norvegicus* peroxisomal membrane protein 2 (PXMP2) were used to obtain fluorescent fusion proteins theoretically targeted to the insect cell nucleus, secretion pathway, Golgi apparatus, lysosomes, nuclear envelope and peroxisomes, respectively. Additionally, the *Spodoptera frugiperda* coding sequences for the diuretic hormone receptor (DHR) and actin (ACT) were amplified from Sf9 cells by reverse transcriptase (RT)-PCR and engineered as above to obtain fluorescent markers of plasma membrane and actin cytoskeleton, respectively. The sequences of these isolated *S. frugiperda* genes were deposited in the GenBank database under the accession codes HQ008729 (DHR) and HQ008727 (ACT). In addition, a synthetic mCherry construct containing endoplasmic reticulum (ER) signalling and retention sequences (Nelson *et al.*, 2007) was used as an ER red fluorescent marker. A summary of all the engineered fluorescent organelle markers is presented in Table 1.

All engineered fluorescent markers were expressed in Sf9 cells and their distribution was visualized by live imaging using confocal laser microscopy (Fig. 3A). The subcellular distribution of the engineered markers agreed to what was expected according to the known localization of these proteins. In the case of the rat or human-derived markers, the distribution of the lysosomal marker was identical to lysotracker-red stained Sf9 lysosomes (Fig. S1A). Similarly, the peroxisomal marker distributed in numerous small punctuate cytoplasmic structures, such as typical peroxisomes of Sf9 cells (Tscherepanow & Kummert, 2007), that were not stained with Lysotracker-red (Fig. S1B). In addition the patterns of the ER and Golgi network markers were similar to the stained respective organelles as reported in Sf9 cells (Kawar & Jarvis, 2001). Finally, the gene coding for diuretic hormone receptor used as a plasma membrane marker was isolated from Sf9 cells and validated by colocalization with the CellTracker™ CM-DiI from Molecular Probes (Invitrogen) stain (Fig. S1C).

The coexpression and live imaging of different combinations of fluorescent markers was carried out to assess the utility of the vector set for simultaneous imaging of multiple FPs. By adjusting the microscope parameters (ie photomultiplier tube range, sequential scan, laser power,

Table 1. Proteins used for the construction of the set of fluorescent organelle markers

Symbol	Gene name	Origin	Subcellular localization	GenBank accession no.
LMNA	Lamin C	*Homo sapiens*	Nucleus	NM_005572
TGOLN2	Trans Golgi network protein 2	*H. sapiens*	Golgi network	NM_006464
PLA2G15	Phospholipase A2	*H. sapiens*	Lysosomes	NM_012320
KDELR1	KDEL endoplasmic reticulum retention receptor 1	*H. sapiens*	Secretion pathway	NM_006801
PXMP2	Peroxisomal membrane protein 2	*Rattus norvegicus*	Peroxisomes	NM_031587
TOR1AIP1	Torsin A interacting protein 1	*R. norvegicus*	Nuclear envelope	NM_145092
ER-mCherry	*A. thaliana* WAK2 gene signal peptide/mCherry/KDEL retention signal as in Nelson *et al*. (2007)	Synthetic	Endoplasmic reticulum	
ACT	Actin	*Spodoptera frugiperda*	Actin cytoskeleton	HQ008727
DHR	Diuretic hormone receptor	*S. frugiperda*	Plasma membrane	HQ008729

scanning frequency, pinhole diameter, etc.), the separate acquisition of up to three different FPs emissions in the same sample was possible (Fig. 3B). Even when using three different vectors simultaneously, the majority of the transfected cells showed expression of all the fluorescent proteins assayed (data not shown). As expected, upon coexpression of the ER, Golgi network and secretory pathway fluorescent markers, partial colocalization between the ER and the Golgi network as well as between the Golgi network and the secretory pathway was observed (Fig. 3C), further validating the correct distribution of these organelle markers.

Illustration of the use of the vector set for in vivo *colocalization studies*

In order to reveal the usefulness of the vector set for the rapid *in vivo* subcellular localization of a protein of interest within insect cells, fluorescent fusions to the MRCV major outer capsid protein P10 (Distéfano *et al*., 2005) were constructed and their subcellular distribution was analysed by colocalization with some of the organelle markers described above. Upon expressing the P10:GFP fluorescent fusion in Sf9 cells, a cytoplasmic distribution was observed (Fig. 4A). In contrast, the N-terminal fluorescent fusion of P10 was able to colocalize with the ER marker (Fig. 4B), thus suggesting that the ER localization depends on a free MRCV P10 C-terminal end.

Example of the use of the vector set for in vivo *self-interaction studies*

Taking advantage of the self-interaction capacity of MRCV P9-1 (Maroniche *et al*., 2010), the usefulness of the vector set in FRET studies was evaluated using CFP/YFP pairs as the donor/acceptor couple. The CFP:P9-1 and P9-1:YFP fusions were coexpressed in Sf9 cells for subsequent live imaging and FRET calculations by the acceptor sensitized emission method (Brzostowski *et al*., 2009). The P9-1 fluorescent fusions showed donor to acceptor energy transfer localizing principally in the inclusion bodies where both proteins were present (Fig. 5A). In contrast, no energy transfer was detected when CFP and YFP were coexpressed simultaneously as an interaction negative control (Fig. 5B). In conclusion, our results show that this novel set of vectors is suitable for simultaneously studying *in vivo* protein–protein interactions and subcellular distribution, by live imaging and FRET.

Discussion

Construction and evaluation of a vector set for live imaging in insect cells

The determination of several complete insect genomes has led to an increasing need to study protein function (Grimmelikhuijzen *et al*., 2007). Live imaging is a widely used methodology based on the use of FPs for real time studies of protein behaviour within the living cell. Using this technique, it is possible to determine subcellular localization, interactions, kinetics and many other properties of proteins in their natural environment (Day & Schaufele, 2005). In particular, live imaging technology is a powerful strategy to study insect proteins during larval development (Cavey & Lecuit, 2008). Insect expression vectors for protein live imaging in several species have been engineered (Huynh & Zieler, 1999), in some cases combining the fast and easy Gateway cloning technology that relies on highly efficient homologous recombination reactions (Hartley *et al*., 2000). For example, *Drosophila melanogaster* P-element based Gateway destination vectors designed for expression of GFP and mRFP fusion proteins in transgenic flies have been developed (Akbari *et al*., 2009). Likewise, a set of three Gateway destination vectors designed to express GFP and DsRed-based fluorescent fusion proteins in *Bombyx mori* and other lepidopteran cells has been developed and tested using several proteins (Mitsunobu *et al*., 2006). In this work, we followed this approach to develop a collection of eight Gateway destination vectors useful for *in vivo* protein subcellular localization in insect cells. The vectors were designed to express a protein of interest fused to any of

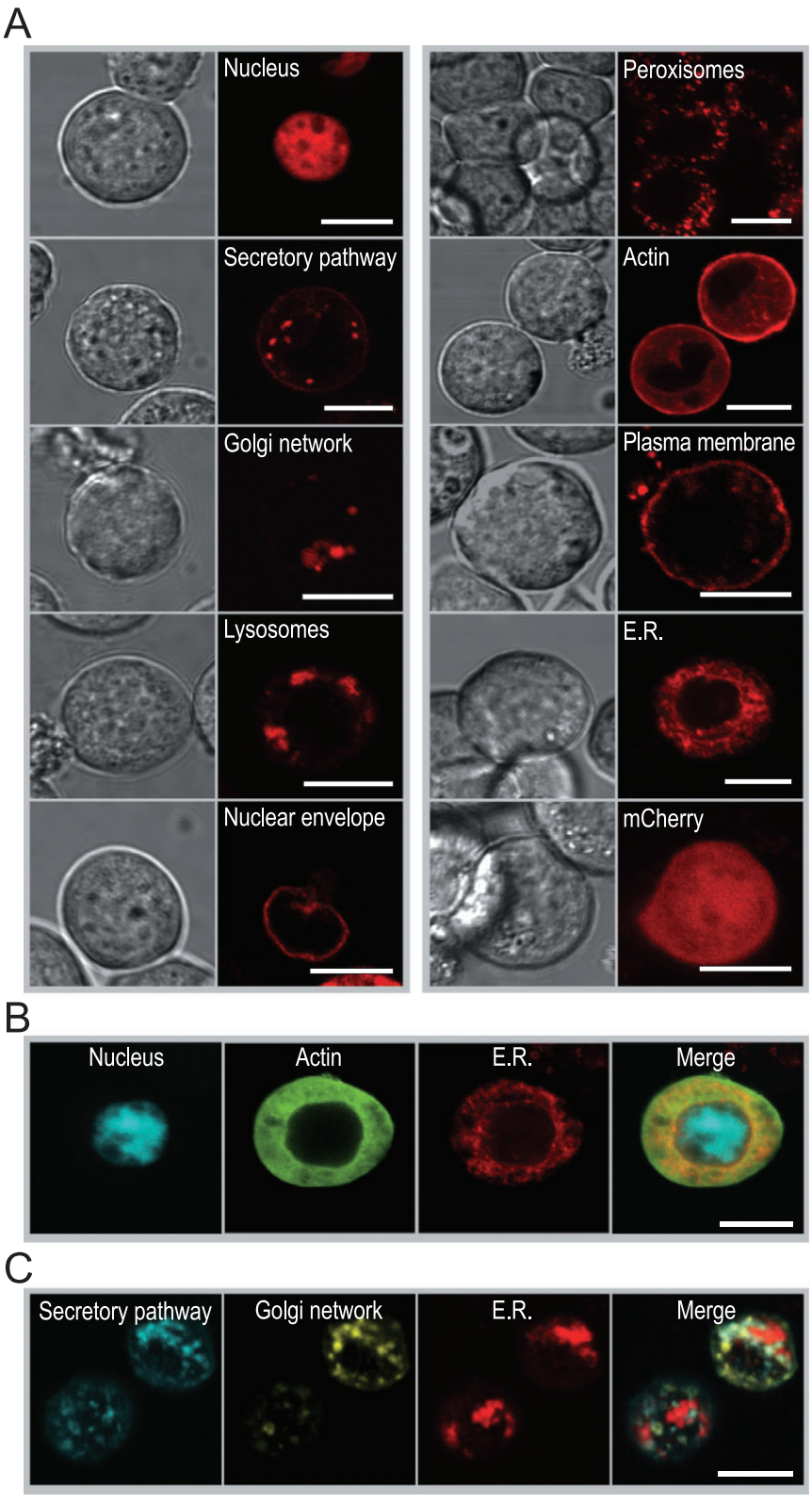

Figure 3. Live imaging of *Spodoptera frugiperda* Sf9 cells (Sf9) expressing the collection of fluorescent organelle markers fused to mCherry assembled in this work. (A) The gene coding sequences of *Homo sapiens* lamin C (LMNA), KDELR1, TGOLN2 and PLA2G15, *Rattus norvegicus* TOR1AIP1 and PXMP2, *Spodoptera frugiperda* ACT and DHR and the synthetic ER-mCherry, were used to obtain reference fluorescent proteins (FPs) targeted to the nucleus, secretion pathway, Golgi network, lysosomes, nuclear envelope, peroxisomes, actin cytoskeleton, plasma membrane and endoplasmic reticulum (ER), respectively. Their subcellular localization in Sf9 cells was analysed by acquiring images of the marker fluorescence (right panels) and the bright field (left panels). The nonfused mCherry protein was expressed from the pIB-RW vector as a control (bottom right). (B) Multiple labelling was carried out by coexpressing the fluorescent markers LMNA1:CFP (nucleus), YFP:ACT (actin) and ER:mCherry (ER) in Sf9 cells. The images correspond to the fluorescent markers and to the merging of all three fluorescent images. (C) Coexpression of the KDELR1:CFP (secretory pathway), TGOLN2:YFP (Golgi network) and ER:mCherry (ER) fluorescent markers in Sf9 cells showing partial colocalization of the markers (Merge). Scale bars = 10 μm. See Table 1 for the definition of all the genes used.

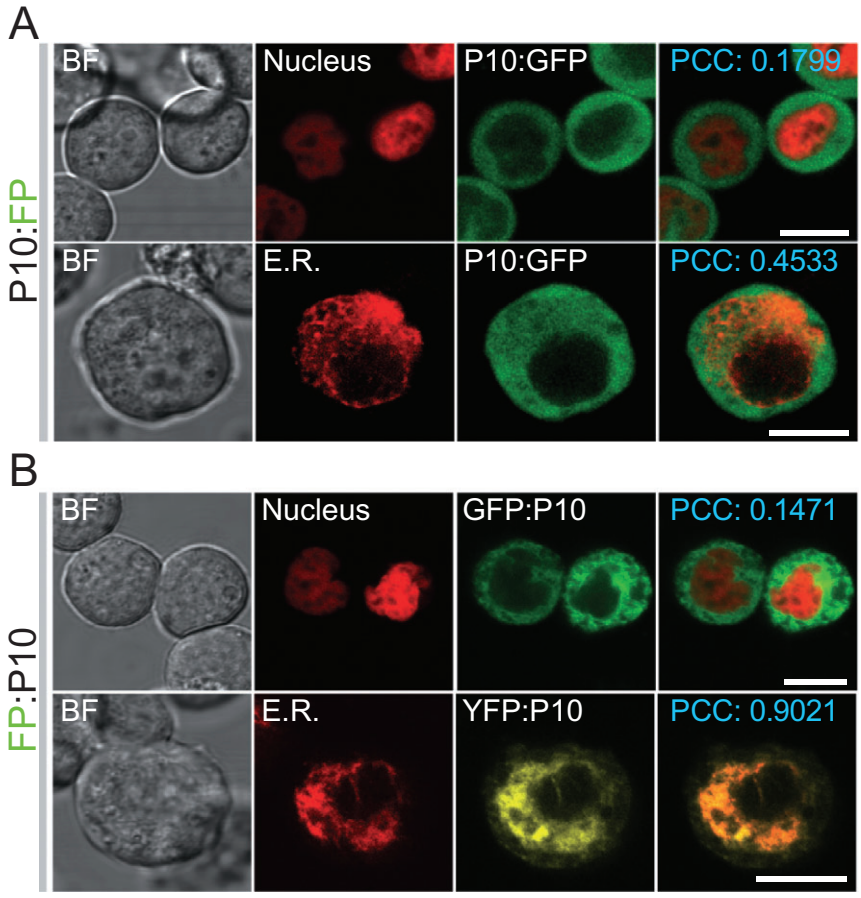

Figure 4. Analysis of *Mal de Río Cuarto virus* (MRCV) P10 subcellular localization. Fluorescent fusions of the MRCV P10 protein, constructed by fusing fluorescent proteins (FPs) to the C-terminal (A) and N-terminal (B) ends, were transiently expressed in *Spodoptera frugiperda* Sf9 cells (Sf9) and analysed by live imaging. Images of the cells under the bright field (BF), of two mCherry-based fluorescent reference markers [nucleus or endoplasmic reticulum (ER)] and of the P10 fluorescent fusions, are shown. Both fluorescent signals were then merged (far right panel) and the colocalization of the FPs was examined by calculating the Pearson's correlation coefficient (PCC). Scale bars = 10 μm.

four different FPs (GFP, CFP, YFP and mCherry) by either its C-terminal or N-terminal end. The monomeric red fluorescent mCherry protein was selected for its improved features over the tetrameric DsRed parental protein (Shaner *et al*., 2004). The expression of each resulting fluorescent fusion protein is driven by the constitutive *Orgyia pseudotsugata multicapsid nucleopolyhedrosis virus* (OpMNPV) immediate-early 2 gene promoter (pOpIE2). This promoter was chosen because it is active in many commonly used lepidopteran and dipteran insect cell lines (Pfeifer *et al*., 1997; Lee *et al*., 2008) and is not as strong as baculovirus late promoters such as the polyhedrin promoter or very late promoters such as p10 promoter (Jarvis *et al*., 1990). This point was taken ito account because over-expression could be a problem in some cases when defining protein subcellular localization upon transfection. Importantly, during this work we did not detect alternative localizations of a given protein as would be expected if there was a protein over-expression artefact. It is also important to highlight that, unlike baculoviral

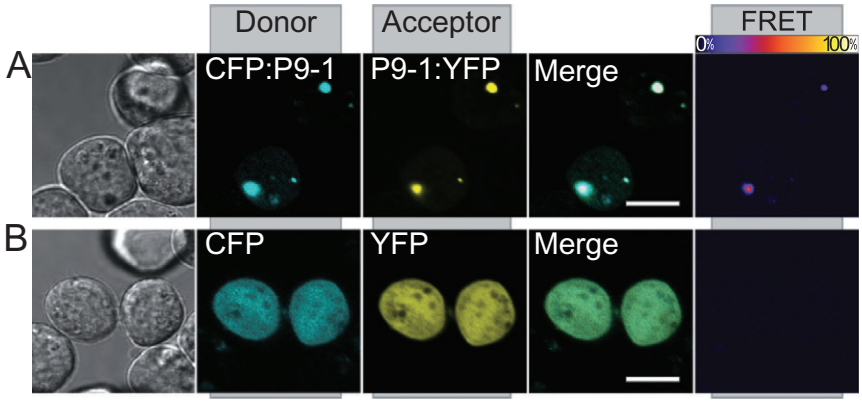

Figure 5. Analysis of *Mal de Río Cuarto virus* (MRCV) P9-1 *in vivo* self-interaction by Förster resonance energy transfer (FRET). The MRCV P9-1 fluorescent fusions CFP:P9-1 and P9-1:YFP were coexpressed in *Spodoptera frugiperda* Sf9 cells (Sf9) and their *in vivo* interaction was assayed by FRET using the acceptor sensitized emission method (A). In parallel, CFP and YFP proteins were used as a negative interaction control (B). Samples separately expressing CFP or YFP were used for bleed-through corrections (data not shown). The images of the bright field, fluorescent proteins (FPs; donor and acceptor), the fluorescence merge and the FRET index (as calculated by the acceptor sensitized emission method), are shown. Scale bars = 10 μm.

mediated expression of proteins in lepidopteran cells, the vector set presented here is a more reliable system for protein subcellular localization because it circumvents possible interference effects or artefacts resulting from the baculovirus infection itself.

An evaluation of the correct functionality of the developed vector set was carried using the MRCV P9-1 protein. This protein was chosen because it displays an unambiguous inclusion body-forming property when expressed in Sf9 cells (Maroniche *et al*., 2010). Upon obtaining fluorescent fusions of P9-1, expressing them in Sf9 cells and analysing their distribution by live imaging, the GFP, YFP and CFP-based P9-1 fluorescent fusions were located in bright fluorescent cytoplasmic inclusions. By contrast, the two mCherry fusions to P9-1 did not form inclusions but were instead dispersed in the cell cytoplasm with some occasional accumulations. This could be the result of a change in P9-1 structure or functionality by the fusion to mCherry somehow affecting its ability to self-interact, as we did not detect differences in the subcellular localization of the reference markers when fused to mCherry or GFP (data not shown). Nevertheless, the results indicate that this novel vector set is functional and adequate to express fluorescent fusions of proteins in insect cells, and that it is highly advisable to use different fluorescent fusion partners when studying subcellular localization of proteins.

In order to assign precisely the subcellular localization of a protein, colocalization analyses using reference markers are essential. Specific fluorescent stains are mostly used when fixation of cells is required for subsequent immunofluorescence experiments. By contrast, in live imaging experiments it is more appropriate to coexpress FPs of known distribution as a reference. In this case, it is necessary to rely on several fluorescent markers fused to proteins that target common cellular compartments and structures and whose spectra do not overlap with the spectrum of the fusion protein of interest. Consequently, the vector set developed during this work was used to engineer a set of specific fluorescent markers targeted to several organelles and cellular structures. The expected subcellular localization of the fluorescent markers expressed in Sf9 cells was verified by live imaging and in some cases by colocalization with organelle specific stains. Further experiments were carried out to test the suitability of the vector collection for multiple labelling studies. Live multiple labelling is a powerful technique for analysing the *in vivo* behaviour of several proteins simultaneously, but it requires the use of FPs with minimal spectral overlapping properties. Our results show that the new vector set is useful for multiple labelling studies in live insect cells because three different FPs (CFP, YFP and mCherry) emissions could be separately acquired. Still, with the proper image processing such as spectral unmixing (Falk & Lauf, 2001; Dinant *et al*., 2008), it might be possible to detect simultaneously the four different FPs.

Deployment of the vector set for in vivo *subcellular localization and FRET*

MRCV, a member of the *Fijivirus* genus that belongs to the *Reoviridae* family (Distefano *et al*., 2002), is a plant-infecting virus that is able to replicate both in plants and planthoppers of the family *Delphacidae* (Milne *et al*., 2005). The members of this genus have been poorly studied at the molecular level partly because of the lack of planthopper cell lines and because viral proteins are difficult to express in heterologous systems such as bacteria and model plant species. The vector set constructed during this work was used to establish the subcellular localization of MRCV P10 protein. MRCV P10 has 72.4% identity to the *Rice black streaked dwarf virus* (RBSDV) major outer capsid protein (Distéfano *et al*., 2005). In turn, RBSDV P10 was shown to self-interact by its N-terminal domain forming trimers (Liu *et al*., 2007). Fluorescent fusions of MRCV P10 were expressed in Sf9 cells and examined by live imaging. Surprisingly, the N-terminal P10 fluorescent fusions were targeted to the ER although no signals for ER targeting or retention could be detected in MRCV P10 sequence by bioinformatic analyses. These results suggested that P10 is able to target the ER by an unknown mechanism that might involve a direct penetration into the ER membrane or the external attachment of P10 to this structure. By contrast, fusion of the FP partner to the MRCV P10 C-terminal end resulted in a cytoplasmic localization of the quimeric protein, indicating that the C-terminal end of MRCV P10 might be involved in the ER localization. The observed P10 distribution in the ER might reflect the *Fijivirus* requirement of the ER membrane system for viral morphogenesis, as has been demonstrated for members of the *Rotavirus* genus (Pesavento *et al*., 2006). Moreover, cytoplasmic tubular structures that sometimes show a membranous aspect and contain mature virus particles are frequently observed in cells infected with MRCV and other fijiviruses (Bassi & Favali, 1972; Isogai *et al*., 1998; Arneodo *et al*., 2002), suggesting that the cell endomembrane system might be connected with the formation of such structures. Thus, our results suggest that MRCV P10 could be involved in the exploitation of ER membranes during the viral replication cycle or in mediating the association of the mature virus particles to these tubular structures. The localization of *Fijivirus* outer capsid protein at the ER has not been noted before and its implications for virus infection will be studied in the future. Importantly, the results presented here show that the vector system developed during this work is a highly valuable tool that can uncover new characteristics of a protein of interest by analysing its subcellular localization. In addition, the results evidence

the importance of always expressing the protein of interest fused to a FP at both protein ends because different results could be obtained in each case.

Like other reoviruses' viroplasm matrix proteins, MRCV P9-1 exhibits a strong self-interaction capacity (Maroniche *et al*., 2010). This P9-1 feature might be locally required during viroplasm formation for the establishment of a macromolecular structure that serves as a scaffold. This hypothesis was tested using P9-1 fusions to YFP and CFP in a FRET assay. As expected, the P9-1 fluorescent fusions were able to self-interact principally in the inclusion bodies. These results show that the novel vectors are well suited for studying *in vivo* interaction of proteins. Although CFP and YFP were chosen because they are the most widely used FRET pair, the vector set reported here has great potential for FRET studies using other successfully tested FRET pairs such as GFP/YFP or GFP/mCherry (Tramier *et al*., 2006; Dinant *et al*., 2008; Albertazzi *et al*., 2009).

In conclusion, the engineered Gateway vector set developed during this work proved to be adequate for rapid functional characterization of a protein of interest by subcellular localization and *in vivo* interaction with a test partner. Thus, it stands as a powerful tool for high-throughput protein functional analysis by live imaging in insect cells.

Experimental procedures

Plasmid construction

The coding sequences of GFP, YFP and CFP were amplified from vectors pEGFP, pEYFP and pECFP (Clontech, Mountain View, CA, USA), respectively, by PCR using primers GFPH-F (5′- AAGCTTATGGTGAGCAAGGGCGAGGAGCTG-3′) and GFPH-s/stop-R (5′- AAGCTTGTACAGCTCGTCCATGCCG AGAG-3′) that exclude the termination codon and add *Hind*III restriction sites (underlined), or primers GFPX-F (5′- TCTAGA GATGGTGAGCAAGGGCGAGGAGCTG-3′) and GFPX-R (5′- TCTAGAGTACAGCTCGTCCATGCCGAGAG-3′) that add flanking *Xba*I recognition sites (underlined). Likewise, the mCherry open reading frame was amplified from pRBCherry (R. Baltanas, unpubl. data) using primers mCherryH-F (5′- AAGCTTATGGTTAGTAAAGGAGAAG-3′) and mCherryH-s/stop-R (5′-AAGCTTTCTAGATCCGGTGGATCCCG-3′) or primers mCherryX-s/atg-F (5′-TCTAGAGGTTAGTAAAGGAGAAG-3′) and mCherryX-R (5′-TCTAGATTACCTGGATCCGGTGGA TCCC-3′), to yield a *Hind*III flanked sequence that lacks a termination codon in the first case and a *Xba*I flanked sequence in the second case.

All of the amplified sequences were cloned in pCR8/GW/TOPO (Invitrogen, Carlsbad, CA, USA) and automatically sequenced to control their correct assembly. The resulting vectors carrying the sequences with the *Hind*III sites were named pTg-GFPH, pTg-YFPH, pTg-CFPH and pTg-mCherryH, and the vectors carrying the sequences without an initiation codon and flanked by *Xba*I sites were named pTg-GFPX, pTg-YFPX, pTg-CFPX and pTg-mCherryX. The first four vectors were digested with *Hind*III and the last four with *Xba*I, and the resulting inserts were subcloned into *Hind*III or *Xba*I treated pIB-V5/His-DEST (Invitrogen) vector, respectively. The resulting Gateway destination vectors were named pIB-GW, pIB-YW, pIB-CW, pIB-RW, pIB-WG, pIB-WY, pIB-WC and pIB-WR, and sequenced to check for the correct assembly of all reading frames.

To obtain MRCV P9-1 N-terminal fluorescence fusions, the entry vector Tg-P9-1s/atg (Maroniche *et al*., 2010) containing the P9-1 coding sequence without the ATG initiation codon was recombined into the destination vectors pIB-GW, pIB-YW, pIB-CW and pIB-RW using the Gateway system (Invitrogen), giving rise to pIB-G-P9-1, pIB-Y-P9-1, pIB-C-P9-1 and pIB-R-P9-1 vectors, respectively. The MRCV P9-1 C-terminal fusions were constructed in the same way by recombining pTg-P9-1s/stop (Maroniche *et al*., 2010), that contains the P9-1 coding sequence lacking the termination codon, into pIB-WG, pIB-WY, pIB-WC and pIB-WR, giving rise to pIB-P9-1-G, pIB-P9-1-Y, pIB-P9-1-C and pIB-P9-1-R, respectively.

For the construction of some of the organelle fluorescent markers, entry vectors containing the coding sequences of LMNA (NM_005572), KDELR1 (NM_006801), TGOLN2 (NM_006464), Tor1aip1 (NM_145092), Pxmp2 (NM_031587), and PLA2G15 (NM_012320) genes lacking their termination codons (kindly supplied by Dr Stefan Wiemann) were transferred by recombination to pIB-WR or pIB-WC destination vectors. The LMNA sequence used in this work codes for a deleted version of the original *H. sapiens* lamin C (GenBank: NP_005563.1) lacking the first 150 amino acids.

For the isolation of the actin cytoskeleton and plasma membrane marker genes used in this work, total RNA was extracted from Sf9 cells with the RNAqueous kit (Ambion, Austin, TX, USA) and used for cDNA synthesis with Superscript III (Invitrogen) and oligo(dT) primers. Using this cDNA as a template, the actin and diuretic hormone receptor coding regions were amplified by PCR using the primers Sf.Act-S/ATG-F (5′-TGCGA CGACGATGTTGCTG-3′) and Sf.Act-R (5′-TTAGAAGCACTTG CGGTGG3′), and Sf.Dhr-F (5′-ATGTGCGACGACGATGTTG CTG-3′) and Sf.Dhr-S/STOP-R (5′-TTATACCGTGAGTCGTAT GCTTTC-3′) primer pairs, respectively, that were designed from available *Spodoptera exigua* and *S. frugiperda* sequences (GenBank accession codes: AY507963 and FJ374694). Finally, the endoplasmic reticulum marker was isolated from the pBin-ER-rb vector (Nelson *et al*., 2007) using primers ER-mCherry-FW (5′-ATGAAGGTACAGGAGGGTTTG-3′) and ER-mCherry-RV (5′-TTACAGCTCGTCTTTAGATCTC-3′). The four amplified sequences were cloned into pCR8/GW/TOPO (Invitrogen) and sequenced, and the resulting entry vectors were used for recombination with pIB-RW (for the actin cytoskeletal marker), pIB-WR (for the plasma membrane marker) or pIB/V5-His-DEST (for the endoplasmic reticulum marker), giving rise to pIB-R-Act, pIB-Dhr-R and pIB-ER expression vectors.

For the construction of MRCV P10 expression vectors, the coding sequence of P10 was amplified by RT-PCR from cDNA synthesized from total RNA of MRCV-infected maize as explained before, using the primer pair 5′-GCTGATATAAGACTCGACA TAG-3′/5′-TCATCTAACAACTTTGTTACATACA-3′ that excludes the initiation codon or the primer pair 5′-ATTATGGCTGATATA AGACTCGACA-3′/5′-TCTAACAACTTTGTTACATACAAC-3′ that excludes the termination codon of this gene. The amplified fragments were cloned in pCR8/GW/TOPO (Invitrogen), sequenced

and subsequently transferred to the appropriate destination vectors by Gateway recombination to obtain P10 fluorescent fusion expression vectors.

Cell culture and transfection

Spodoptera frugiperda Sf9 (IPLBSF21-AE clonal isolate 9) cells were seeded into 35 mm Glass Bottom Culture Dishes (MatTek Corporation, Ashland, MA, USA) using Sf900II Serum free media medium (Invitrogen) supplemented with 2% foetal bovine serum (Invitrogen), and incubated at 27 °C until 60–70% confluence. Cells were then transfected with 1 μg of each plasmid using Cellfectin transfection reagent (Invitrogen) according to the manufacturer's instructions, and incubated at 27 °C until live imaging.

Fluorescent live imaging

At 72 h post-transfection, the culture medium was replaced with phosphate buffered saline pH 6.2 and transfected cells were used for fluorescent imaging in a Leica TCS-SP5 (Leica Microsystems GmbH, Wetzlar, Germany) spectral laser confocal microscope using a 63× objective (HCX PL APO CS 63.0 × 1.20 WATER UV). The 458, 488 and 514 nm lines of the Argon laser were used for CFP, GFP and YFP excitation, respectively, and the 543 nm line from the HeNe laser was employed for mCherry excitation. Scanning was performed in sequential mode to minimize signal bleed-through, and fluorescence emission was detected with the following channel settings: 465–505 nm for CFP, 498–540 nm for GFP, 525–600 nm for YFP and 610–670 nm for mCherry. The microscope power settings, detectors gain and scanning speed were adjusted to optimize contrast and resolution for each individual image. The FPs' colocalizations were determined by calculating the Pearson's correlation coefficient with the colocalization module of the Leica LAS AF software.

FRET

All FRET analyses were computed by the sensitized emission protocol from Regions Of Interest adjusted to individual cells and using the FRET Analyzer plug-in (Hachet-Haas *et al*., 2006) of ImageJ software. The bleed-through correction was performed using images collected from cells expressing only the donor or only the acceptor protein. All the images used for analysis were generated using identical microscope parameters [ie zoom, laser power, Photomultiplier tubes, acousto-optic tunable filter transmission, detectors gain, scanning speed].

Acknowledgements

All vectors are available upon request for research purposes only. We are grateful to Dr Stefan Wiemann from the Division of Molecular Genome Analysis of the German Cancer Research Center for providing several human and rat organelle markers. This work was supported by research projects PICT 2006 n°. 0358 from the Argentine Agency for Promotion of Science and Technology (ANPCyT) and PE AEBIO-244621 from the National Institute of Agronomic Technology (INTA). G. A. M., V. C. M. and G. L. hold doctoral fellowships from the Consejo Nacional de Investigaciones Científicas y Técnicas (CONICET). V. A., O. T. and M. d. V. are career members of CONICET. The authors would like to thank Dr Sebastián Asurmendi and Dr Marcelo Berretta for critical reading of the manuscript.

References

Adams, M.D., Celniker, S.E., Holt, R.A., Evans, C.A., Gocayne, J.D., Amanatides, P.G. *et al*. (2000) The genome sequence of *Drosophila melanogaster*. *Science* **287**: 2185–2195.

Akbari, O., Oliver, D., Eyer, K. and Pai, C.-Y. (2009) An Entry/Gateway(R) cloning system for general expression of genes with molecular tags in Drosophila melanogaster. *BMC Cell Biol* **10**: 8.

Albertazzi, L., Arosio, D., Marchetti, L., Ricci, F. and Beltram, F. (2009) Quantitative FRET analysis with the EGFP-mCherry fluorescent protein pair. *Photochem Photobiol* **85**: 287–297.

Arneodo, J.D., Lorenzo, E., Laguna, I.G., Abdala, G. and Truol, G.A. (2002) Cytopathological characterization of Mal de Río Cuarto virus in corn, wheat and barley. *Fitopatol Bras* **27**: 298–302.

Bassi, M. and Favali, M.A. (1972) Electron microscopy of Maize rough dwarf virus assembly sites in maize. Cytochemical and autoradiographic observations. *J Gen Virol* **16**: 153–160.

Brzostowski, J.A., Meckel, T., Hong, J., Chen, A. and Jin, T. (2009) Imaging protein-protein interactions by Forster resonance energy transfer (FRET) microscopy in live cells. *Curr Protoc Protein Sci* **19**: Unit19 5.

Cavey, M. and Lecuit, T. (2008) Imaging cellular and molecular dynamics in live embryos using fluorescent proteins. *Methods Mol Biol* **420**: 219–238.

Cole, N.B., Smith, C.L., Sciaky, N., Terasaki, M., Edidin, M. and Lippincott-Schwartz, J. (1996) Diffusional mobility of Golgi proteins in membranes of living cells. *Science* **273**: 797–801.

Day, R.N. and Schaufele, F. (2005) Imaging molecular interactions in living cells. *Mol Endocrinol* **19**: 1675–1686.

Dinant, C., Van Royen, M.E., Vermeulen, W. and Houtsmuller, A.B. (2008) Fluorescence resonance energy transfer of GFP and YFP by spectral imaging and quantitative acceptor photobleaching. *J Microsc* **231**: 97–104.

Distefano, A.J., Conci, L.R., Munoz Hidalgo, M., Guzman, F.A., Hopp, H.E. and del Vas, M. (2002) Sequence analysis of genome segments S4 and S8 of Mal de Rio Cuarto virus (MRCV): evidence that the virus should be a separate *Fijivirus* species. *Arch Virol* **147**: 1699–1709.

Distéfano, A.J., Hopp, H.E. and del Vas, M. (2005) Sequence analysis of genome segments S5 and S10 of Mal de Rio Cuarto virus (*Fijivirus*, *Reoviridae*). *Arch Virol* **150**: 1241–1248.

Eisenhaber, F. and Bork, P. (1998) Wanted: subcellular localization of proteins based on sequence. *Trends Cell Biol* **8**: 169–170.

Falk, M.M. and Lauf, U. (2001) High resolution, fluorescence deconvolution microscopy and tagging with the autofluorescent tracers CFP, GFP, and YFP to study the structural composition of gap junctions in living cells. *Microsc Res Tech* **52**: 251–262.

Grimmelikhuijzen, C.J., Cazzamali, G., Williamson, M. and Hauser, F. (2007) The promise of insect genomics. *Pest Manag Sci* **63**: 413–416.

Hachet-Haas, M., Converset, N., Marchal, O., Matthes, H., Gioria, S., Galzi, J.L. *et al*. (2006) FRET and colocalization analyzer–a method to validate measurements of sensitized emission FRET acquired by confocal microscopy and available as an ImageJ Plug-in. *Microsc Res Tech* **69**: 941–956.

Hanson, G.T., Aggeler, R., Oglesbee, D., Cannon, M., Capaldi, R.A., Tsien, R.Y. *et al*. (2004) Investigating mitochondrial redox potential with redox-sensitive green fluorescent protein indicators. *J Biol Chem* **279**: 13044–13053.

Hartley, J.L., Temple, G.F. and Brasch, M.A. (2000) DNA Cloning Using In Vitro Site-Specific Recombination. *Genome Res* **10**: 1788–1795.

Heim, R., Prasher, D.C. and Tsien, R.Y. (1994) Wavelength mutations and posttranslational autoxidation of green fluorescent protein. *Proc Natl Acad Sci USA* **91**: 12501–12504.

Heim, R., Cubitt, A.B. and Tsien, R.Y. (1995) Improved green fluorescence. *Nature* **373**: 663–664.

Holt, R.A., Subramanian, G.M., Halpern, A., Sutton, G.G., Charlab, R., Nusskern, D.R. *et al*. (2002) The genome sequence of the malaria mosquito *Anopheles gambiae*. *Science* **298**: 129–149.

Hu, C.D., Chinenov, Y. and Kerppola, T.K. (2002) Visualization of interactions among bZIP and Rel family proteins in living cells using bimolecular fluorescence complementation. *Mol Cell* **9**: 789–798.

Huynh, C.Q. and Zieler, H. (1999) Construction of modular and versatile plasmid vectors for the high-level expression of single or multiple genes in insects and insect cell lines. *J Mol Biol* **288**: 13–20.

Isogai, M., Uyeda, I. and Lee, B.C. (1998) Detection and assignment of proteins encoded by rice black streaked dwarf fijivirus S7, S8, S9 and S10. *J Gen Virol* **79**: 1487–1494.

Jarvis, D.L., Fleming, J.-A.G.W., Kovacs, G.R., Summers, M.D. and Guarino, L.A. (1990) Use of early baculovirus promoters for continuous expression and efficient processing of foreign gene products in stably transformed lepidopteran cells. *Nat Biotechnol* **8**: 950–955.

Kawar, Z. and Jarvis, D.L. (2001) Biosynthesis and subcellular localization of a lepidopteran insect alpha 1,2-mannosidase. *Insect Biochem Mol Biol* **31**: 289–297.

Kirkness, E.F., Haas, B.J., Sun, W., Braig, H.R., Perotti, M.A., Clark, J.M. *et al*. (2010) Genome sequences of the human body louse and its primary endosymbiont provide insights into the permanent parasitic lifestyle. *Proc Natl Acad Sci USA* **107**: 12168–12173.

Lee, J.M., Takahashi, M., Mon, H., Mitsunobu, H., Koga, K., Kawaguchi, Y. *et al*. (2008) Construction of gene expression systems in insect cell lines using promoters from the silkworm, *Bombyx mori*. *J Biotechnol* **133**: 9–17.

Liu, H., Wei, C., Zhong, Y. and Li, Y. (2007) *Rice black-streaked dwarf virus* outer capsid protein P10 has self-interactions and forms oligomeric complexes in solution. *Virus Res* **127**: 34–42.

Maroniche, G.A., Mongelli, V.C., Peralta, A.V., Distefano, A.J., Llauger, G., Taboga, O.A. *et al*. (2010) Functional and biochemical properties of *Mal de Rio Cuarto virus* (*Fijivirus*, *Reoviridae*) P9-1 viroplasm protein show further similarities to animal reovirus counterparts. *Virus Res* **152**: 96–103.

Matz, M.V., Fradkov, A.F., Labas, Y.A., Savitsky, A.P., Zaraisky, A.G., Markelov, M.L. *et al*. (1999) Fluorescent proteins from nonbioluminescent Anthozoa species. *Nat Biotechnol* **17**: 969–973.

Milne, R.C., Del Vas, M., Harding, R.M., Marzachi, C. and Mertens, P.P.C. (2005) *Fijivirus*. In *Virus Taxonomy – Eighth Report of the International Committee on Taxonomy of Viruses* (Fauquet, C.M., Mayo, M.A., Maniloff, J., Desselberger, U. and Ball, L.A., eds), pp. 534–542. Elsevier/Academic Press, London.

Mita, K., Kasahara, M., Sasaki, S., Nagayasu, Y., Yamada, T., Kanamori, H. *et al*. (2004) The genome sequence of silkworm, *Bombyx mori*. *DNA Res* **11**: 27–35.

Mitsunobu, H., Sakashita, K., Mon, H., Yoshida, H., Man Lee, J., Kawaguchi, Y. *et al*. (2006) Construction of Gateway-based destination vectors for detecting subcellular localization of proteins in the silkworm, *Bombyx mori*. *J Insect Biotechnol Sericol* **75**: 141–145.

Miyawaki, A., Griesbeck, O., Heim, R. and Tsien, R.Y. (1999) Dynamic and quantitative Ca2+ measurements using improved cameleons. *Proc Natl Acad Sci USA* **96**: 2135–2140.

Mon, H., Sugahara, R., Hong, S.M., Lee, J.M., Kamachi, Y., Kawaguchi, Y. *et al*. (2009) Analysis of protein interactions with two-hybrid system in cultured insect cells. *Anal Biochem* **392**: 180–182.

Nelson, B.K., Cai, X. and Nebenführ, A. (2007) A multicolored set of *in vivo* organelle markers for co-localization studies in Arabidopsis and other plants. *Plant J* **51**: 1126–1136.

Nene, V., Wortman, J.R., Lawson, D., Haas, B., Kodira, C., Tu, Z.J. *et al*. (2007) Genome sequence of *Aedes aegypti*, a major arbovirus vector. *Science* **316**: 1718–1723.

Pepperkok, R. and Ellenberg, J. (2006) High-throughput fluorescence microscopy for systems biology. *Nat Rev Mol Cell Biol* **7**: 690–696.

Pesavento, J.B., Crawford, S.E., Estes, M.K. and Prasad, B.V. (2006) Rotavirus proteins: structure and assembly. *Curr Top Microbiol Immunol* **309**: 189–219.

Pfeifer, T.A., Hegedus, D.D., Grigliatti, T.A. and Theilmann, D.A. (1997) Baculovirus immediate-early promoter-mediated expression of the Zeocin resistance gene for use as a dominant selectable marker in dipteran and lepidopteran insect cell lines. *Gene* **188**: 183–190.

Prasher, D.C., Eckenrode, V.K., Ward, W.W., Prendergast, F.G. and Cormier, M.J. (1992) Primary structure of the *Aequorea victoria* green-fluorescent protein. *Gene* **111**: 229–233.

Richards, S., Gibbs, R.A., Weinstock, G.M., Brown, S.J., Denell, R., Beeman, R.W. *et al*. (2008) The genome of the model beetle and pest *Tribolium castaneum*. *Nature* **452**: 949–955.

Shaner, N.C., Campbell, R.E., Steinbach, P.A., Giepmans, B.N., Palmer, A.E. and Tsien, R.Y. (2004) Improved monomeric red, orange and yellow fluorescent proteins derived from *Discosoma* sp. red fluorescent protein. *Nat Biotechnol* **22**: 1567–1572.

Shaner, N.C., Patterson, G.H. and Davidson, M.W. (2007) Advances in fluorescent protein technology. *J Cell Sci* **120**: 4247–4260.

Shcherbo, D., Merzlyak, E.M., Chepurnykh, T.V., Fradkov, A.F., Ermakova, G.V., Solovieva, E.A. *et al*. (2007) Bright far-red

fluorescent protein for whole-body imaging. *Nat Methods* **4**: 741–746.

The Honeybee Genome Sequencing Consortium (2006) Insights into social insects from the genome of the honeybee *Apis mellifera*. *Nature* **443**: 931–949.

The International Aphid Genomics Consortium (2010) Genome sequence of the pea aphid *Acyrthosiphon pisum*. *PLoS Biol* **8**: e1000313.

Tramier, M., Zahid, M., Mevel, J.C., Masse, M.J. and Coppey-Moisan, M. (2006) Sensitivity of CFP/YFP and GFP/mCherry pairs to donor photobleaching on FRET determination by fluorescence lifetime imaging microscopy in living cells. *Microsc Res Tech* **69**: 933–939.

Tscherepanow, M. and Kummert, F. (2007) Subcellular localisation of proteins in living cells using a genetic algorithm and an incremental neural network. In *Bildverarbeitung für die Medizin 2007* (Horsch, A., Deserno, T.M., Handels, H., Meinzer, H.-P. and Tolxdorff, T., eds), pp. 11–15. Springer-Verlag, Berlin; Heidelberg.

Werren, J.H., Richards, S., Desjardins, C.A., Niehuis, O., Gadau, J., Colbourne, J.K. *et al*. (2010) Functional and evolutionary insights from the genomes of three parasitoid *Nasonia* species. *Science* **327**: 343–348.

Wong, F.H., Banks, D.S., Abu-Arish, A. and Fradin, C. (2007) A molecular thermometer based on fluorescent protein blinking. *J Am Chem Soc* **129**: 10302–10303.

Wouters, F.S. and Bastiaens, P.I. (1999) Fluorescence lifetime imaging of receptor tyrosine kinase activity in cells. *Curr Biol* **9**: 1127–1130.

Xia, Q., Zhou, Z., Lu, C., Cheng, D., Dai, F., Li, B. *et al*. (2004) A draft sequence for the genome of the domesticated silkworm (*Bombyx mori*). *Science* **306**: 1937–1940.

Supporting Information

Additional Supporting Information may be found in the online version of this article under the DOI reference: 10.1111/j.1365-2583.2011.01100.x

Figure S1. Validation of the targeting of the lysosome, peroxisome and plasma membrane fluorescent markers constructed in this work in insect cells. (A) Sf9 cells were stained with 100 nM Lysotracker Red DND-99 (Invitrogen) for 20 min at room temperature, and the resulting pattern was compared to the one obtained in Sf9 cells expressing the lysosome fluorescent marker. (B) The peroxisome fluorescent marker was expressed in Sf9 cells that were subsequently stained with Lysotracker Red as explained above, and the joint pattern of both fluorophores was analysed. (C) The plasma membrane fluorescent marker was expressed in Sf9 cells that were then subjected to staining with 2 μM CM-DiI (Invitrogen) for 30 min at room temperature, and colocalization of both fluorescent probes was carried out. White bars represent 10 μm.

Please note: Neither the Editors nor Wiley-Blackwell are responsible for the content or functionality of any supporting materials supplied by the authors. Any queries (other than missing material) should be directed to the corresponding author for the article.